

High-Fidelity Simulation of Unsteady Flow Problems using a 3rd Order Hybrid MUSCL/CD scheme

ECCOMAS, June 6th-11th 2016, Crete Island, Greece

A. West & D. Caraeni

Outline

- Industrial Motivation

- Numerical Schemes

- Test Cases:

 - Inviscid Vortex Transport

 - DNS of Taylor-Green Vortices at $Re = 1,600$

 - LES of a Circular Cylinder at $Re = 3,900$

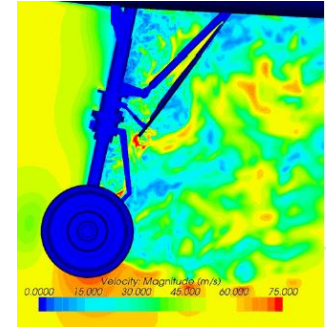
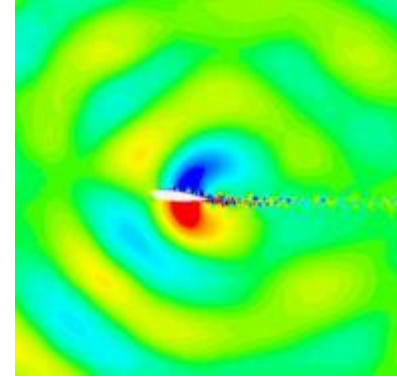
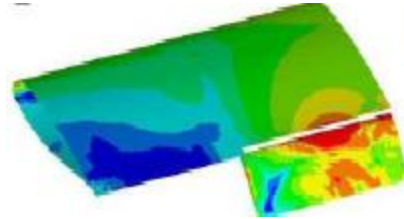
- Conclusions

Industrial Motivation

High-Order CFD targeted for high fidelity simulations

Aerospace

- wing transition,
- high-lift devices
- engine noise
- landing gear aeroacoustics



Automobiles/Trucks

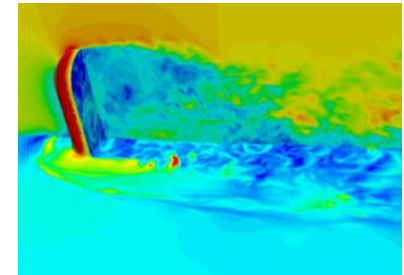
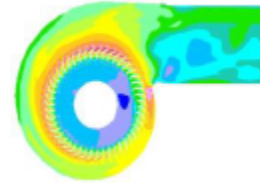
- full vehicle aerodynamics,
- mirror, window, sunroof aeroacoustics,
- HVAC fans, ducts, nozzles, turbochargers

Combustion

- gas turbine, reciprocating engine

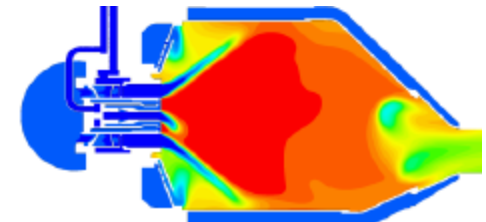
Nuclear (steam line/T-junctions, etc.)

Wind turbines



Numerical solution of (unsteady) turbulent flows requires:

- Accuracy (+ energy conservation, realizability)
- Robustness (large industrial meshes)
- Efficiency (CPU, 10-100 k cores)



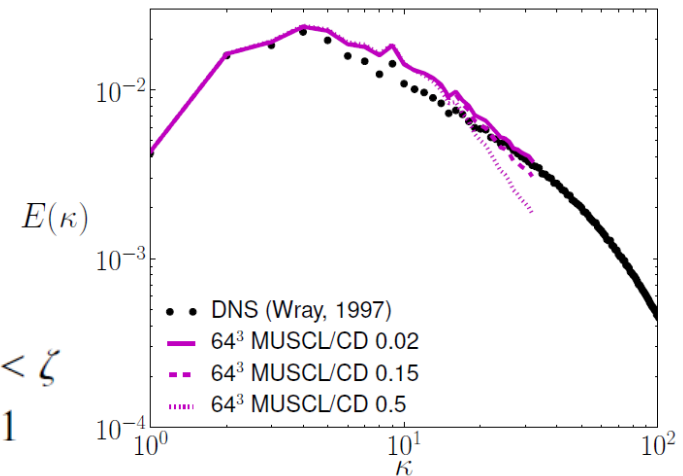
Numerical schemes

- STAR-CCM+, cell-centered FV solver of arbitrary cells
- Two Solvers:
 - Coupled approximate-Riemann solver for all flow regimes
 - Segregated Rhie-Chow SIMPLE or PISO based solver
- Least-Squares gradient reconstruction with high-fidelity gradient limiters
- Preconditioning and other algorithm enhancements for high-fidelity simulations
- BDF 2 and optimized BDF2 (with reduced numerical error) implemented
- LES models (WALE, Smagorinsky and dynamic Smagorinsky)

Convective flux:

- 2nd Order Upwind scheme
- 2nd Order Bounded-CD (hybrid)
- 3rd Order MUSCL/CD scheme (hybrid)

$$(\dot{m}\phi)_f = \begin{cases} \dot{m}\phi_{FOU} & \text{for } \zeta < 0 \text{ or } 1 < \zeta \\ \dot{m}(\sigma\phi_{MUSCL3} + (1 - \sigma)\phi_{CD3}) & \text{for } 0 \leq \zeta \leq 1 \end{cases}$$

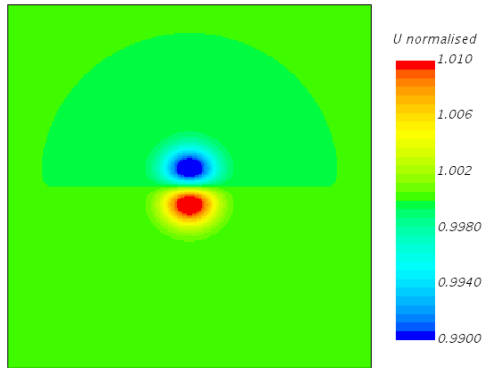


blending based on local smoothness indicator via Normalised Variable Diagram (Darwish et al.)

Inviscid Vortex Transport

“Slow vortex”: $M_\infty = 0.05$, $\beta = 1/50$, $R = 0.005$.

**Initial
Solution
T=0**



$$\delta u = -(U_\infty \beta) \frac{y - Y_c}{R} \exp\left(\frac{-r^2}{2}\right)$$

$$\delta v = (U_\infty \beta) \frac{x - X_c}{R} \exp\left(\frac{-r^2}{2}\right)$$

$$\delta T = \frac{1}{2C_p} (U_\infty \beta)^2 \exp(-r^2)$$

$$u_0 = U_\infty + \delta u$$

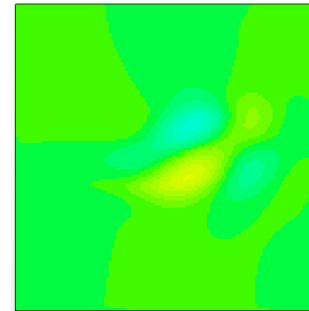
$$v_0 = \delta v$$

$$C_p = \frac{\gamma}{\gamma - 1} R_{\text{gas}}$$

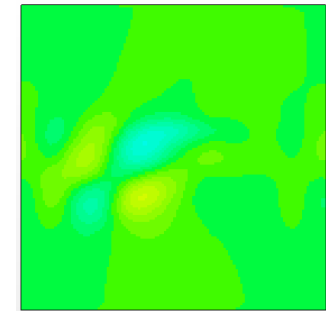
$$r = \frac{\sqrt{(x - X_c)^2 + (y - Y_c)^2}}{R}$$

$$U_\infty = M_\infty \sqrt{\gamma R_{\text{gas}} T_\infty}$$

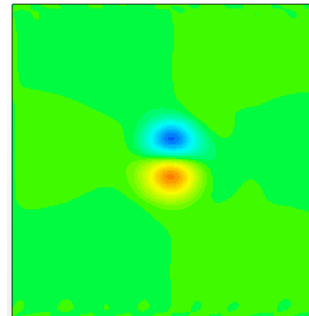
**Solution
T= 50**



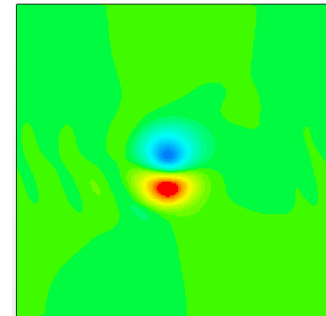
128² 2nd-O upwind



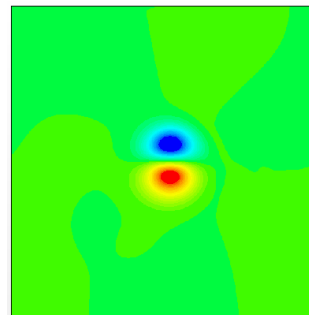
128² 3rd-O MUSCL/CD



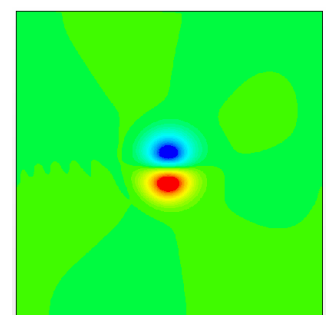
256² 2nd-O upwind



256² 3rd-O MUSCL/CD



512² 2nd-O upwind



512² 3rd-O MUSCL/CD

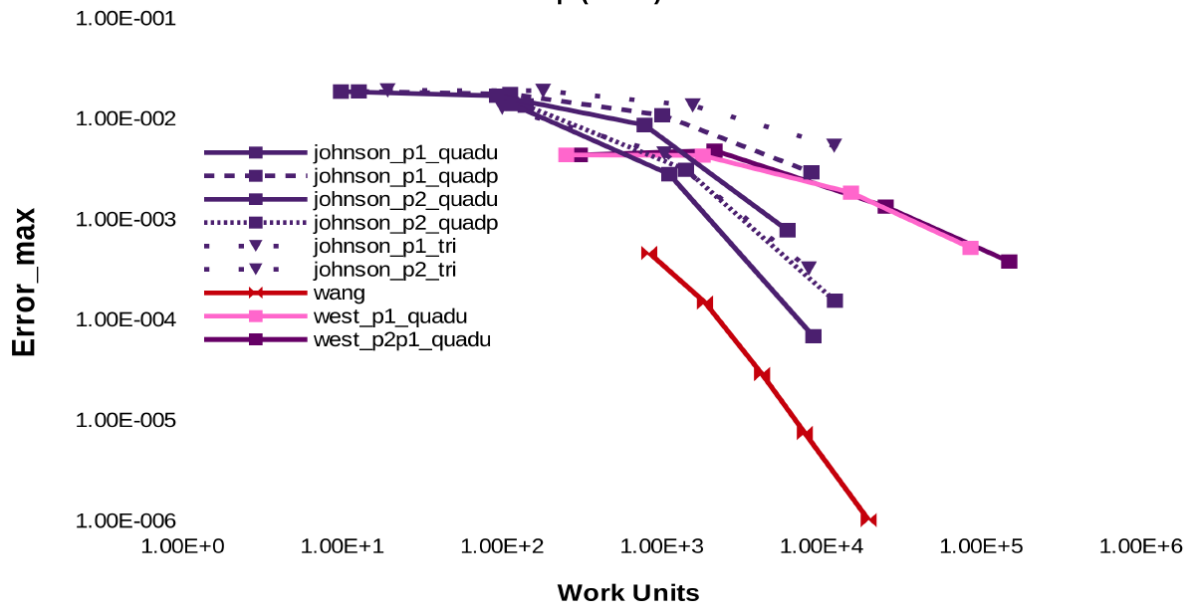
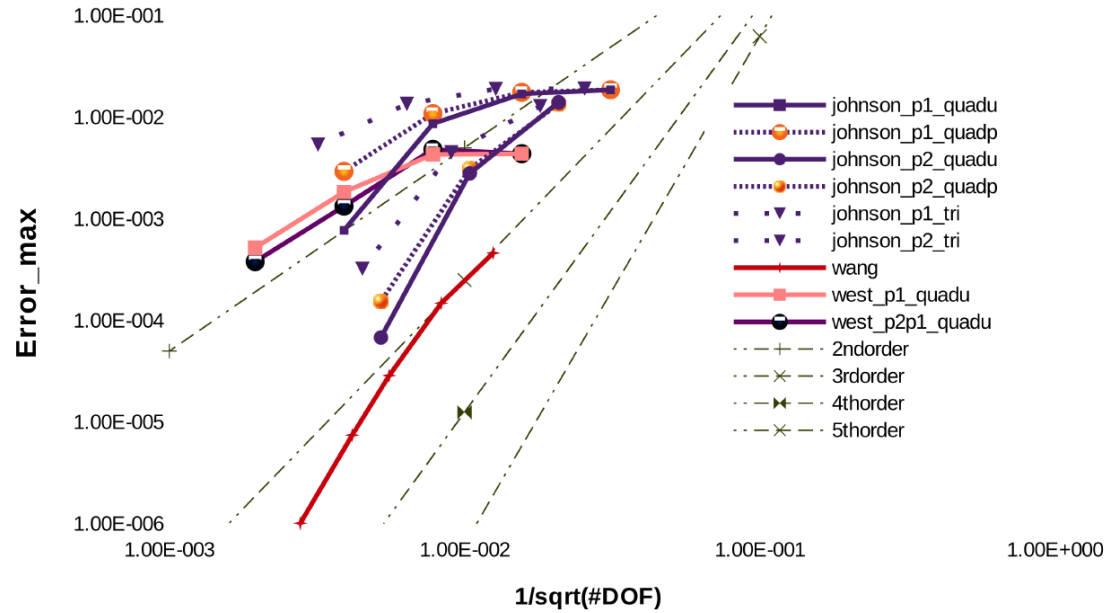
Inviscid Vortex Transport

$$L_2Error_{|U|} = \sqrt{\frac{\sum_{i=1}^N \int_{V_i} (|U| - |U|_{initial})^2 dV}{\sum_{i=1}^N \int_{V_i} dV}}$$

$$|U| = \sqrt{u^2 + v^2}$$

$$WorkUnit = \frac{CPUs \times t_{STAR-CCM+}}{t_{TauBench}}$$

$$h = \frac{1}{\sqrt{nDOF}} = \frac{1}{\sqrt{N}}$$



DNS of Taylor-Green Vortices at Re=1,600

Evolution of quantities:

$$E_k = \frac{1}{\rho_0 \Omega} \int_{\Omega} \rho \frac{\mathbf{v} \cdot \mathbf{v}}{2} d\Omega .$$

$$\epsilon = -\frac{dE_k}{dt} .$$

$$\mathcal{E} = \frac{1}{\rho_0 \Omega} \int_{\Omega} \rho \frac{\boldsymbol{\omega} \cdot \boldsymbol{\omega}}{2} d\Omega .$$

Initial Conditions:

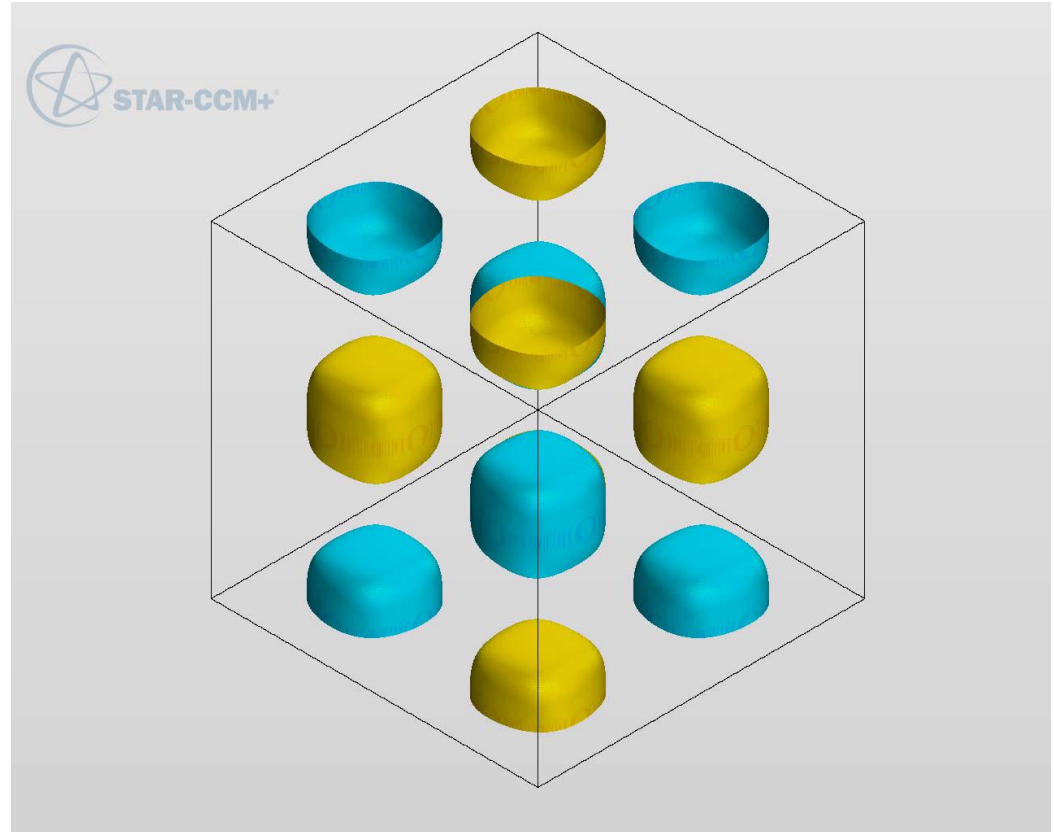
$$u = V_0 \sin\left(\frac{x}{L}\right) \cos\left(\frac{y}{L}\right) \cos\left(\frac{z}{L}\right) ,$$

$$v = -V_0 \cos\left(\frac{x}{L}\right) \sin\left(\frac{y}{L}\right) \cos\left(\frac{z}{L}\right) ,$$

$$w = 0 ,$$

$$p = p_0 + \frac{\rho_0 V_0^2}{16} \left(\cos\left(\frac{2x}{L}\right) + \cos\left(\frac{2y}{L}\right) \right) \left(\cos\left(\frac{2z}{L}\right) + 2 \right) .$$

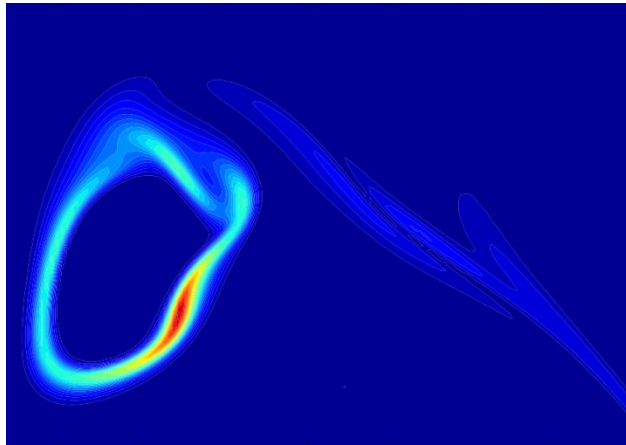
Isosurface of vorticity magnitude coloured by vertical vorticity



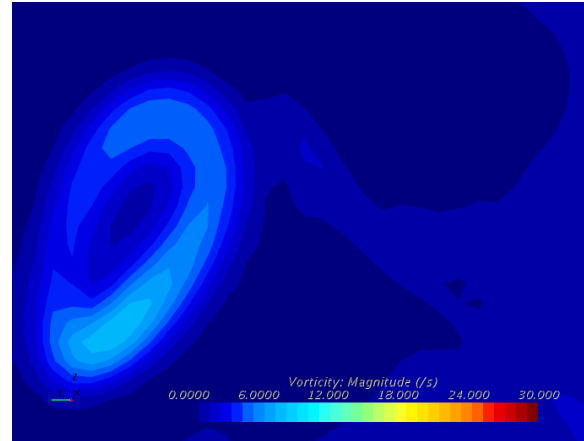
Animation from Patrick McGah

DNS of Taylor-Green Vortices at $Re=1,600$

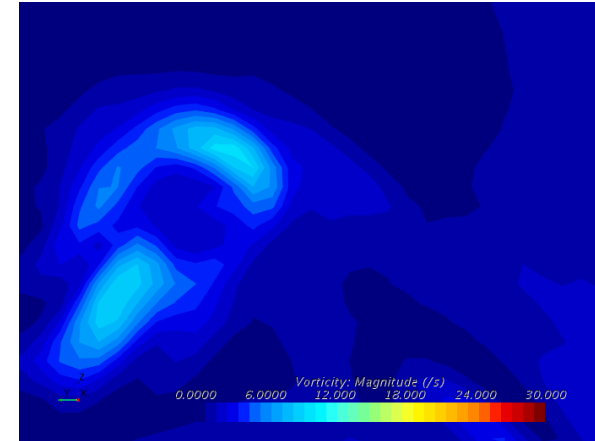
Contours of dimensionless vorticity magnitude $|\omega| L/V_0$ at $x = -\pi L$ and $t_c = 8$.



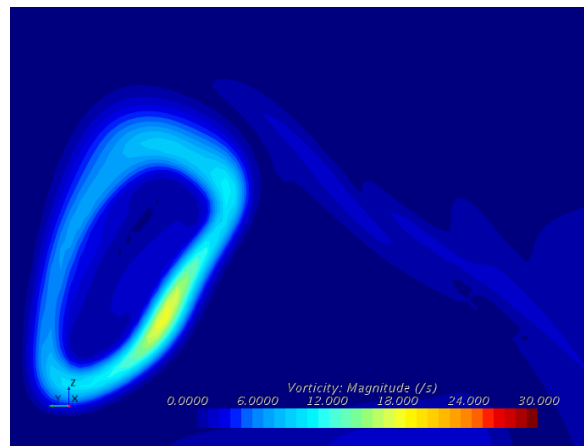
Spectral DNS
(Van Rees et. al, 2011)



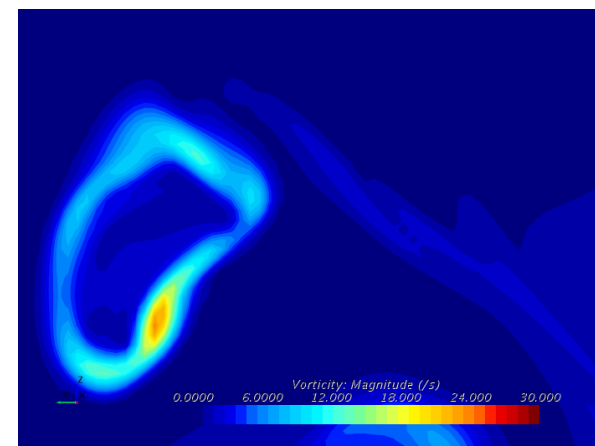
128^3 2nd-O upwind



128^3 3rd-O MUSCL/CD



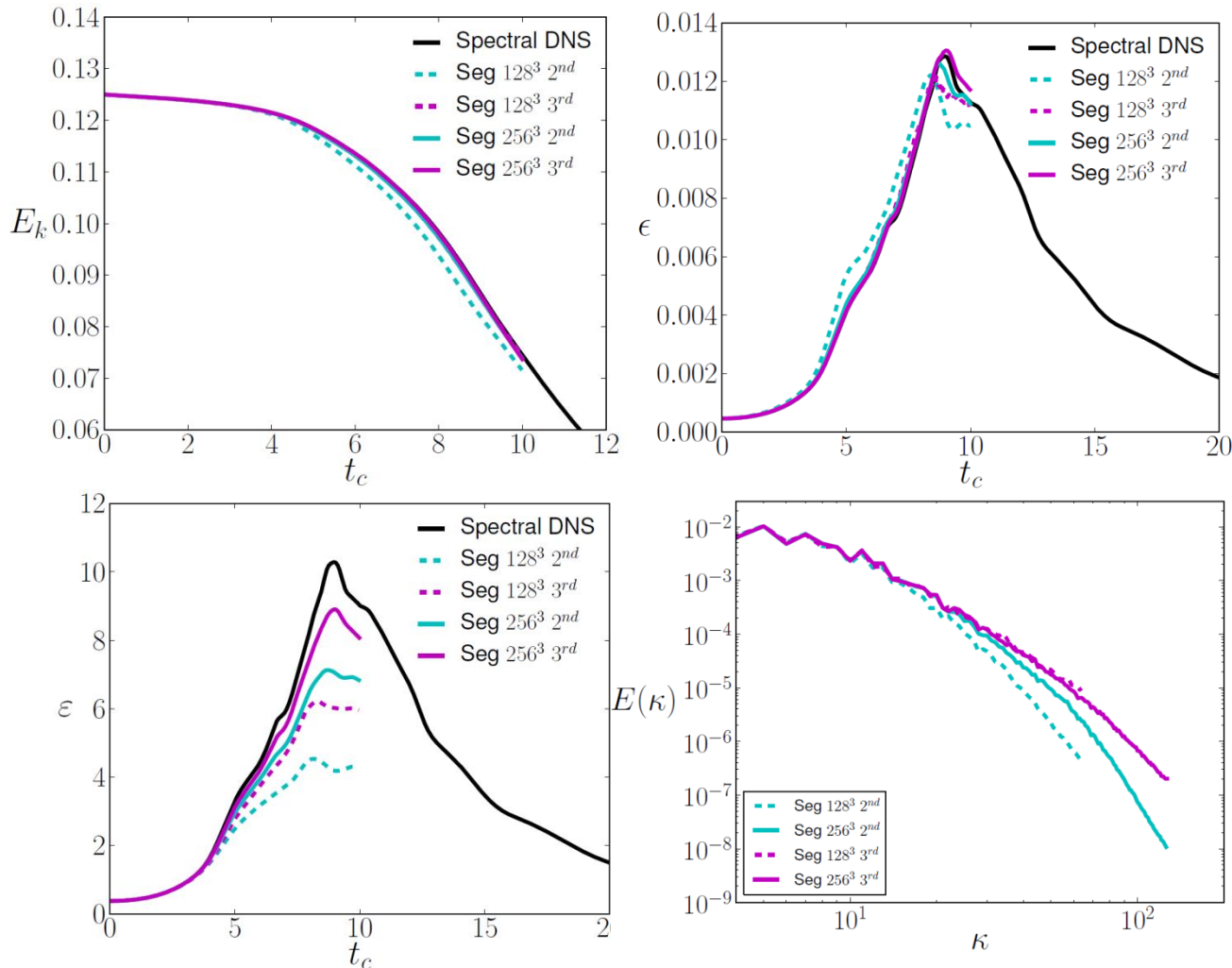
256^3 2nd-O upwind



256^3 3rd-O MUSCL/CD

DNS of Taylor-Green Vortices at Re=1,600

Temporal evolution of total kinetic energy, energy dissipation rate and enstrophy dissipation



$$E_k = \frac{1}{\rho_0 \Omega} \int_{\Omega} \rho \frac{\mathbf{v} \cdot \mathbf{v}}{2} d\Omega .$$

$$\epsilon = -\frac{dE_k}{dt} .$$

$$\mathcal{E} = \frac{1}{\rho_0 \Omega} \int_{\Omega} \rho \frac{\boldsymbol{\omega} \cdot \boldsymbol{\omega}}{2} d\Omega .$$

DNS of Taylor-Green Vortices at Re=1,600

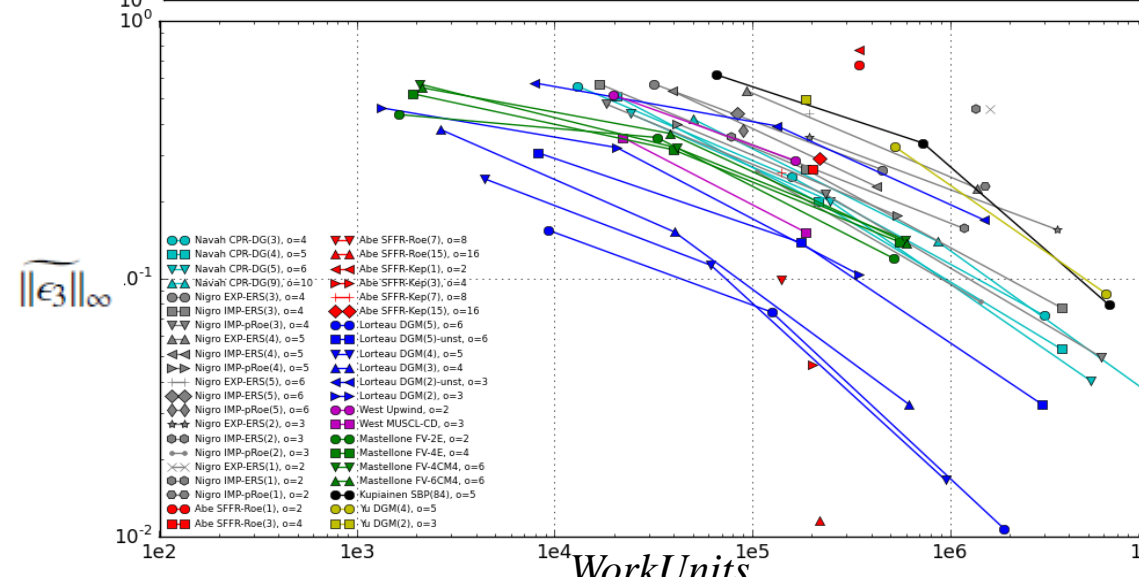
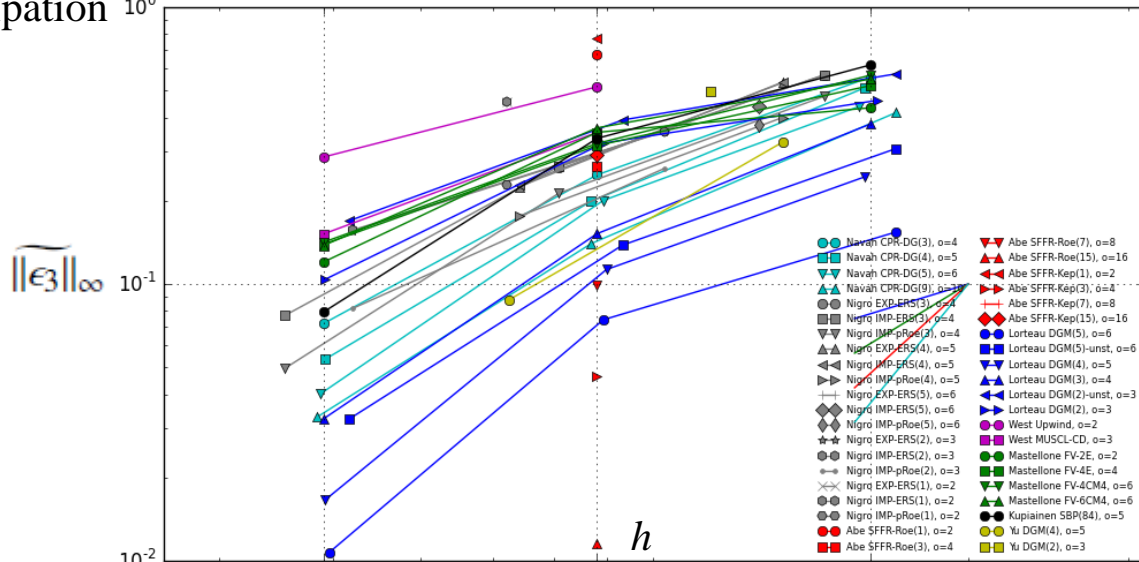
L_∞ error on energy dissipation rate, enstrophy and difference between measured and theoretical dissipation 10^0

$$\|\widetilde{\epsilon}_1\|_\infty = \frac{\left\| \frac{dE_k}{dt} - \left(\frac{dE_k}{dt} \right)^\star \right\|_{t,\infty}}{\max \left(\frac{dE_k}{dt} \right)^\star},$$

$$\|\widetilde{\epsilon}_2\|_\infty = \frac{\left\| 2\nu\varepsilon - 2\nu\varepsilon^\star \right\|_{t,\infty}}{\max \left(\frac{dE_k}{dt} \right)^\star},$$

$$\|\widetilde{\epsilon}_3\|_\infty = \frac{\left\| \frac{dE_k}{dt} - 2\nu\varepsilon \right\|_{t,\infty}}{\max \left(\frac{dE_k}{dt} \right)^\star},$$

$$\|a\|_{t,\infty} = \max_{\epsilon \in [0,10]} |a|.$$



DNS of Taylor-Green Vortices at Re=1,600

L_∞ error on energy dissipation rate, enstrophy and difference between measured and theoretical dissipation 10^0

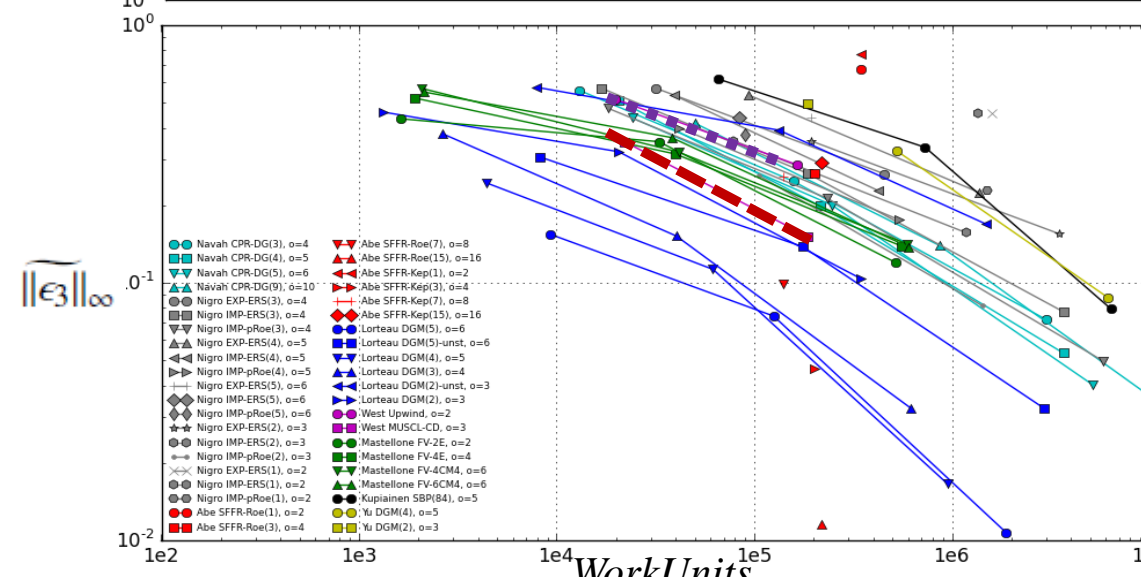
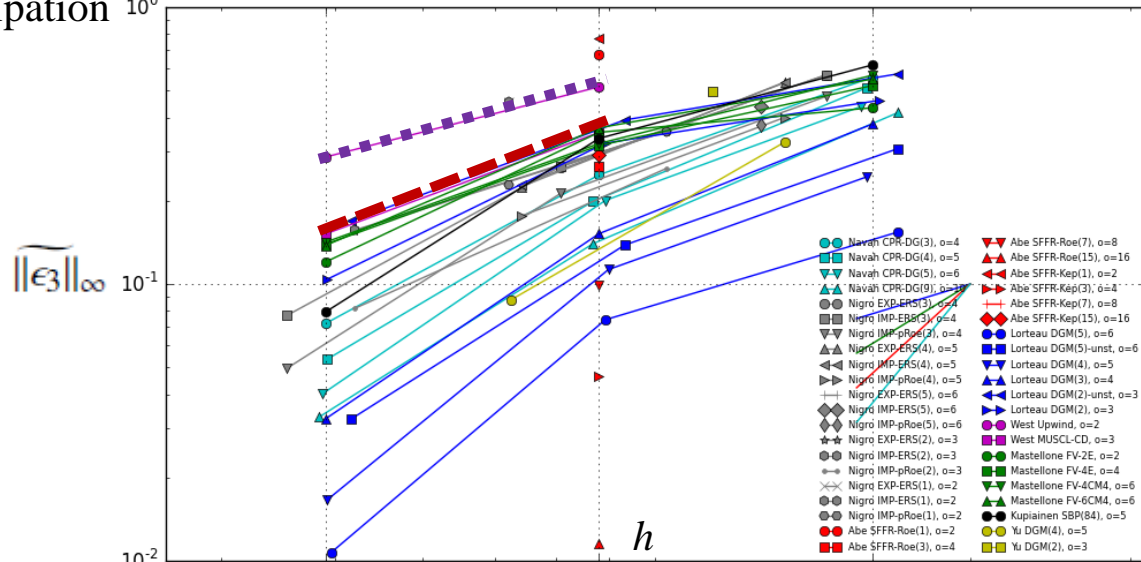
$$\|\widetilde{\epsilon_1}\|_\infty = \frac{\left\| \frac{dE_k}{dt} - \left(\frac{dE_k}{dt}\right)^* \right\|_{t,\infty}}{\max\left(\frac{dE_k}{dt}\right)^*},$$

$$\|\widetilde{\epsilon_2}\|_\infty = \frac{\left\| 2\nu\varepsilon - 2\nu\varepsilon^* \right\|_{t,\infty}}{\max\left(\frac{dE_k}{dt}\right)^*},$$

$$\|\widetilde{\epsilon_3}\|_\infty = \frac{\left\| \frac{dE_k}{dt} - 2\nu\varepsilon \right\|_{t,\infty}}{\max\left(\frac{dE_k}{dt}\right)^*},$$

$$\|a\|_{t,\infty} = \max_{\epsilon \in [0,10]} |a|.$$

■ 2nd-O upwind
■ 3rd-O MUSCL/CD



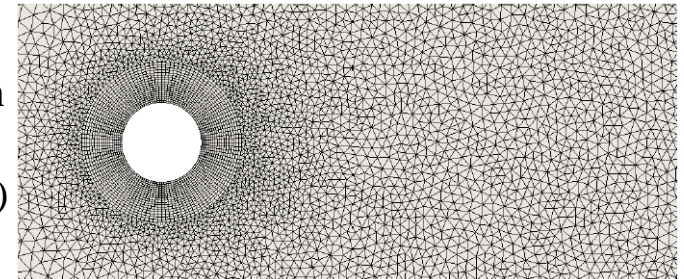
LES of Circular Cylinder at $Re=3,900$

▫ $Ma = 0.2$ $x [-9D, 25D], y [-9D, 9D], z [0, \pi D]$ Coupled implicit solver

▫ periodic in z , free-stream in, pressure outlet for other outer boundaries

▫ Initialised with the Grid-sequencing (solves inviscid flow on coarse-grid levels based on the linear-system coefficients, from coarsest mesh to fine mesh)

Prismatic+
Tetra. HO mesh
(307K, **13.9M**
on P4 elements)



▫ WALE subgrid-scale model (none for PyFR)

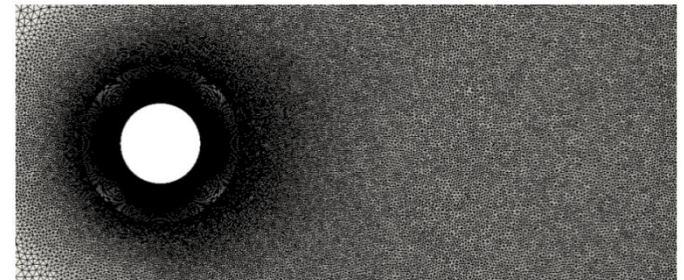
▫ Time statistics collected over 100-1100 t_c

▫ $dt = 8.5e-2 t_c$ (3O)

▫ $dt = 5.0e-3 t_c$ (2O)

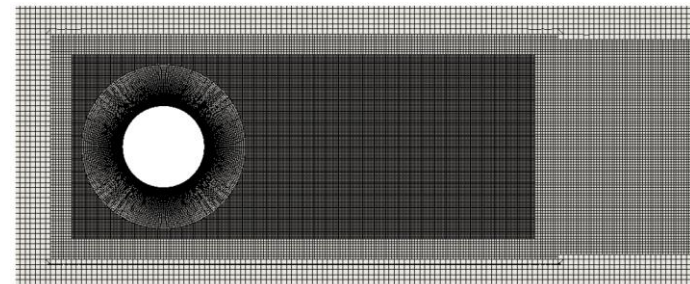
▫ $dt = 2.4e-4 t_c$ (PyFR)

Prismatic+
Tetra. mesh
(**13.2M**)



▫ Ran on 256 cores for 2-3 weeks

Prismatic+
hexa. mesh
(**13.5M**)

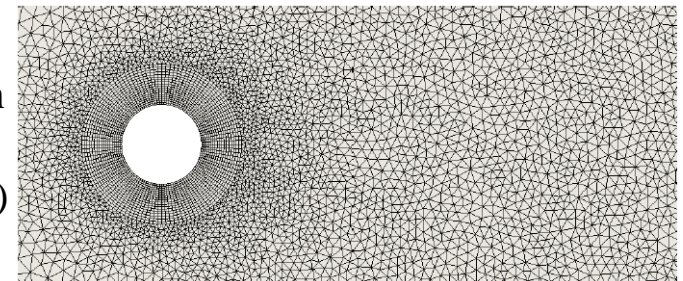


LES of Circular Cylinder at Re=3,900

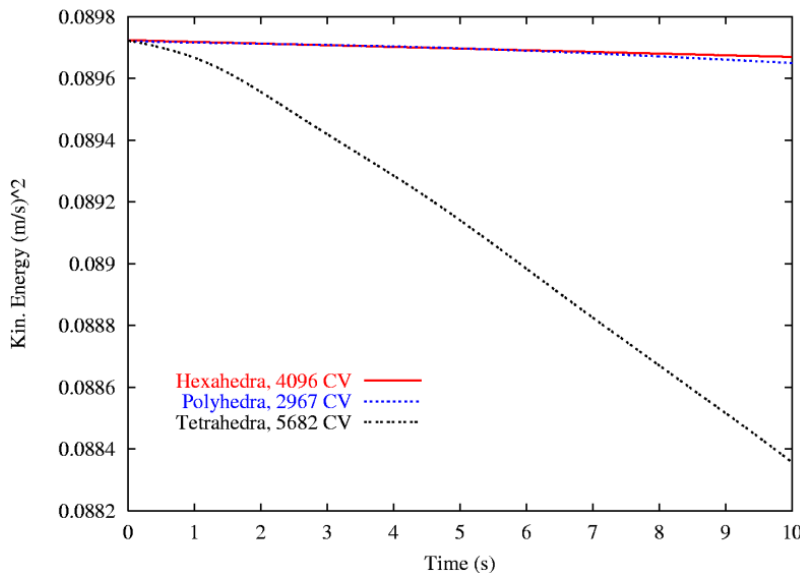
- Ma = 0.2 x [-9D, 25D], y [-9D, 9D], z [0,πD] Coupled implicit solver
- periodic in z, free-stream in, pressure outlet for other outer boundaries

Initialised with the Grid-sequencing (solves inviscid flow on coarse-grid levels based on the linear-system coefficients, from coarsest mesh to fine mesh)

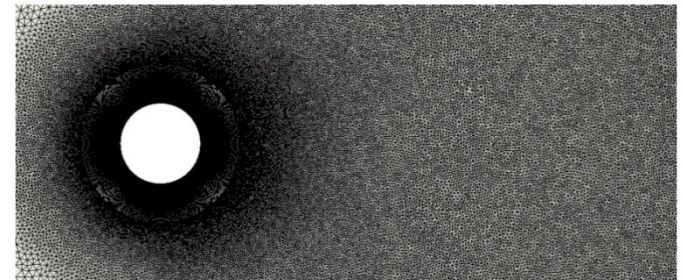
Prismatic+ Tetra. HO mesh (307K, 13.9M elements)



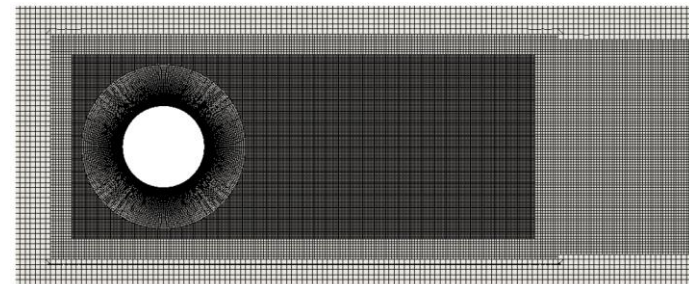
Tetrahedral meshes much more diffusive (see below conservation of kinetic energy for 2D Taylor Green)



Prismatic+ Tetra. mesh (13.2M)



Prismatic+ hexa. mesh (13.5M)

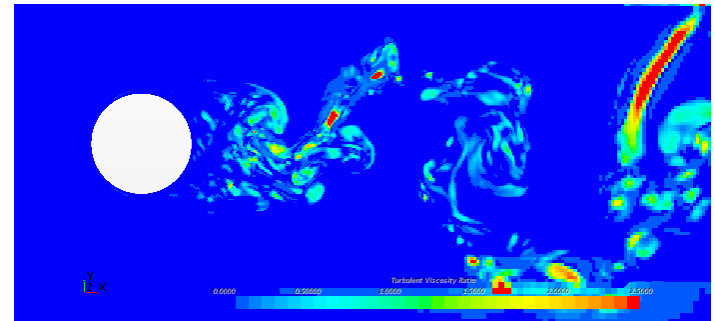
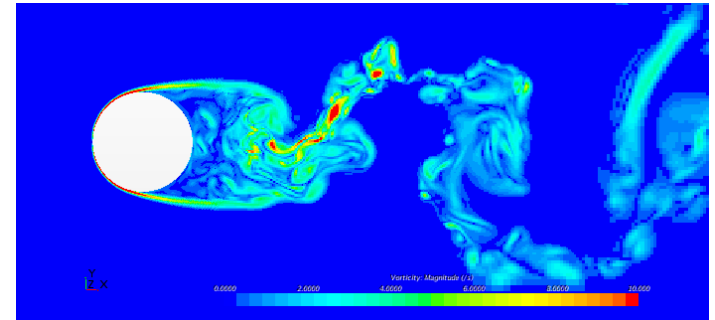
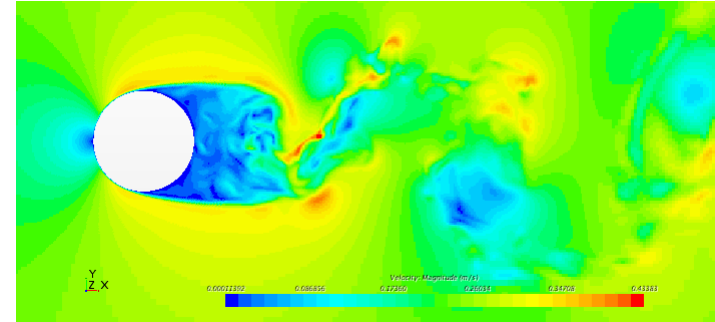


LES of Circular Cylinder at Re=3,900

	L_z/D	$t_c U_\infty/D$	f_{vs}	C_d
Present LES (30 MUSCL/CD)	π	1000	0.215	1.053*
DNS (Lehmkuhl et al. 2013)	π	3900	0.211	1.015
DNS (Ma et al. 2000)	2π	480	0.203	0.96
DNS (Tremblay 2002)	π	240	0.22	1.03
LES (Kravchenko & Moin, 2000)	π	35	0.21	1.04
Exp. (Norberg 1988) (Re=3,000)	67	--	0.22	0.98

* C_d only over 280 t_c

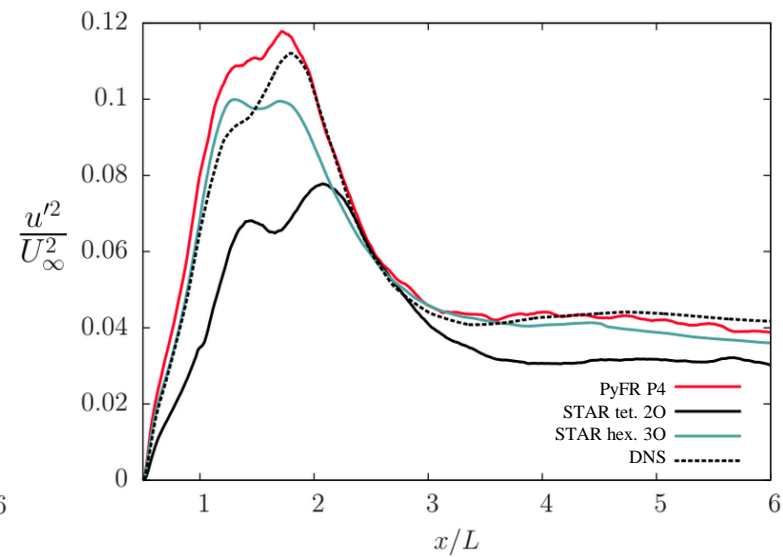
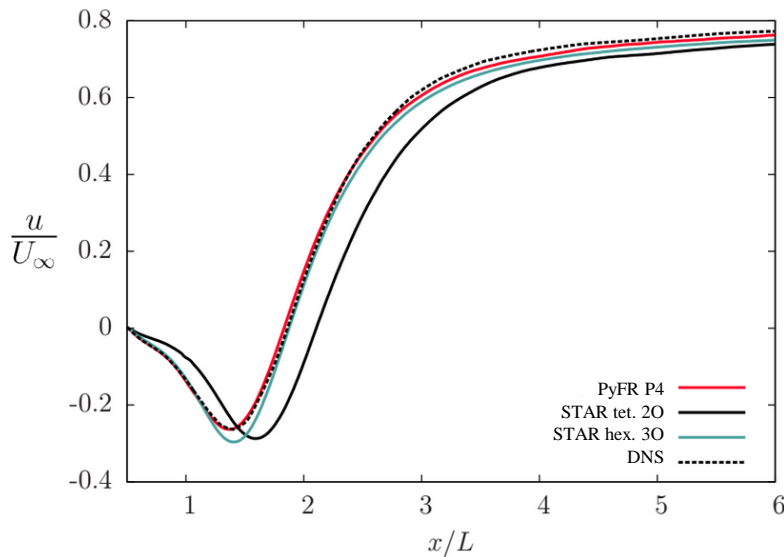
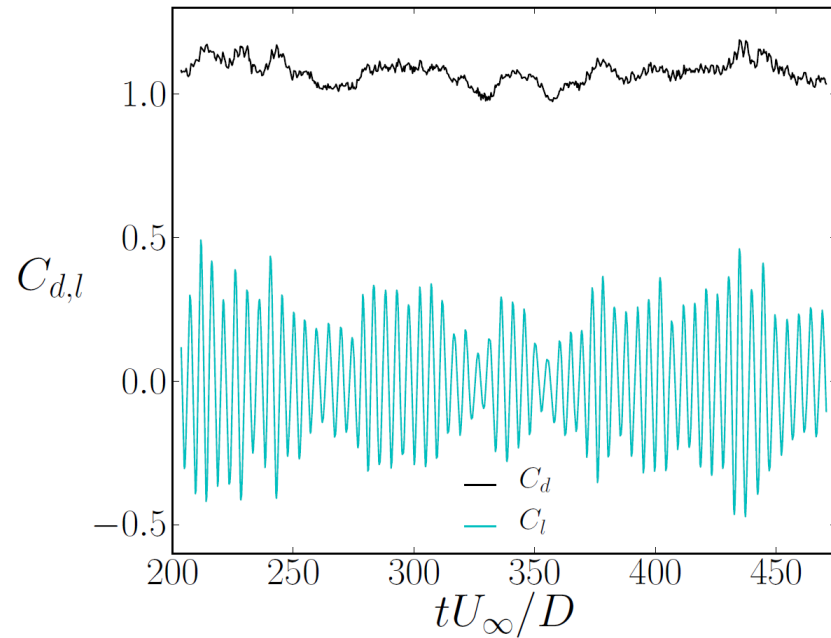
Velocity magnitude, vorticity magnitude & SGS viscosity ratio



LES of Circular Cylinder at $Re=3,900$

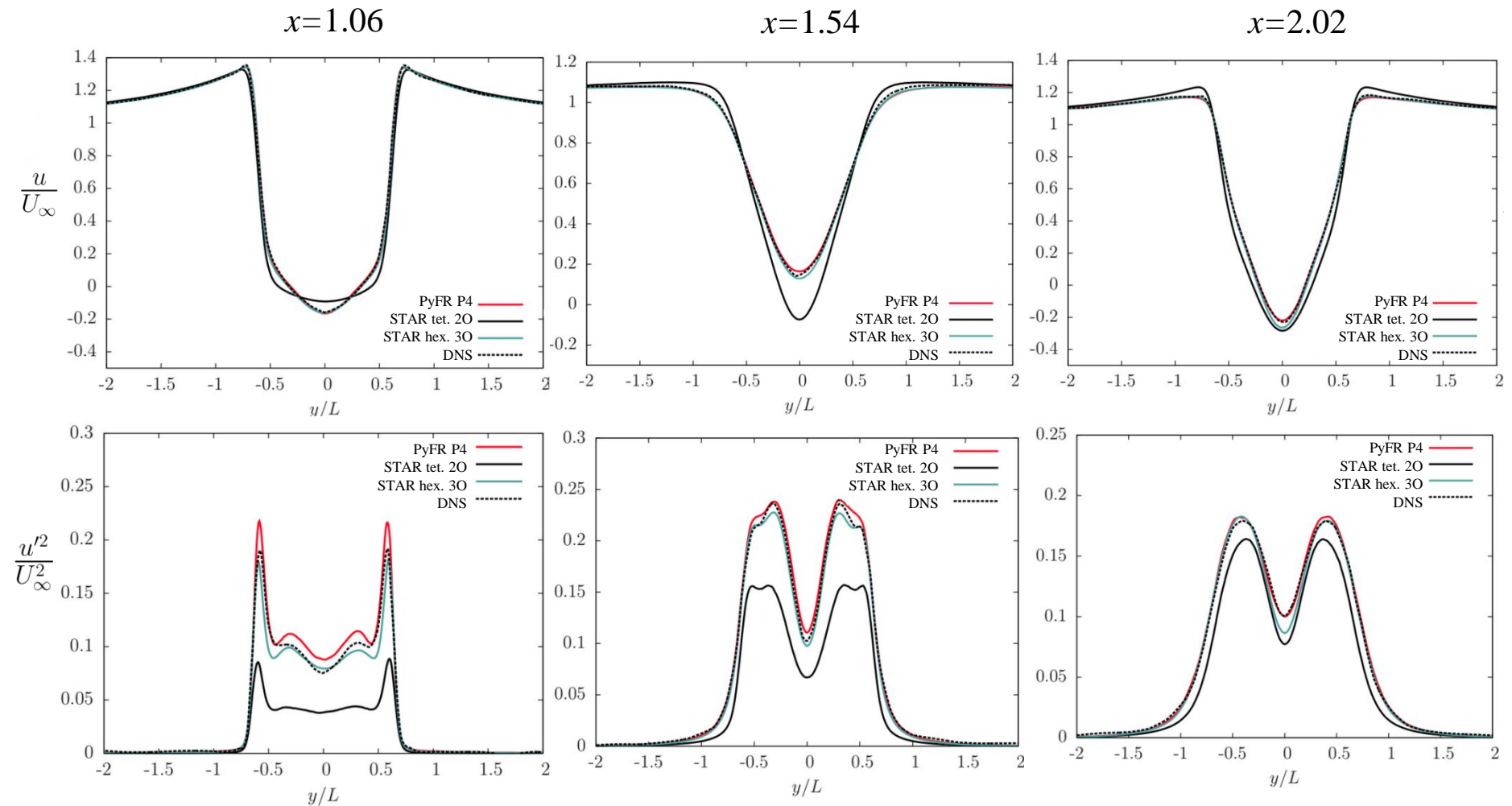
Time evolution of lift and drag showing low-frequency unsteadiness/undulations

Time and Spanwise averaged streamwise velocity and fluctuations along streamwise direction from the cylinder surface



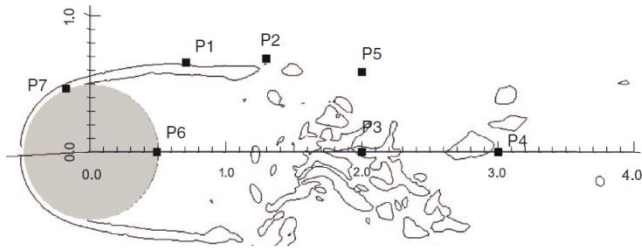
LES of Circular Cylinder at Re=3,900

Time and Spanwise averaged streamwise velocity and fluctuations along streamwise slices

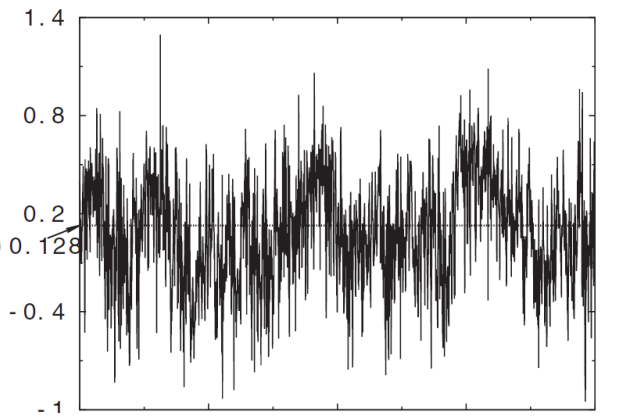


LES of Circular Cylinder at $Re=3,900$

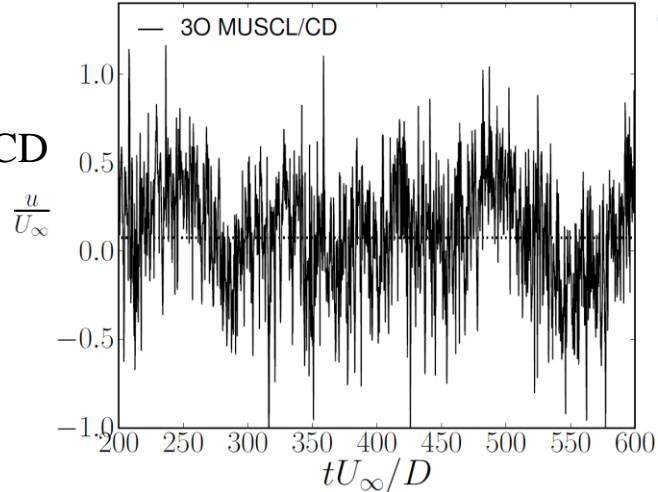
Point velocity fluctuations and spectra



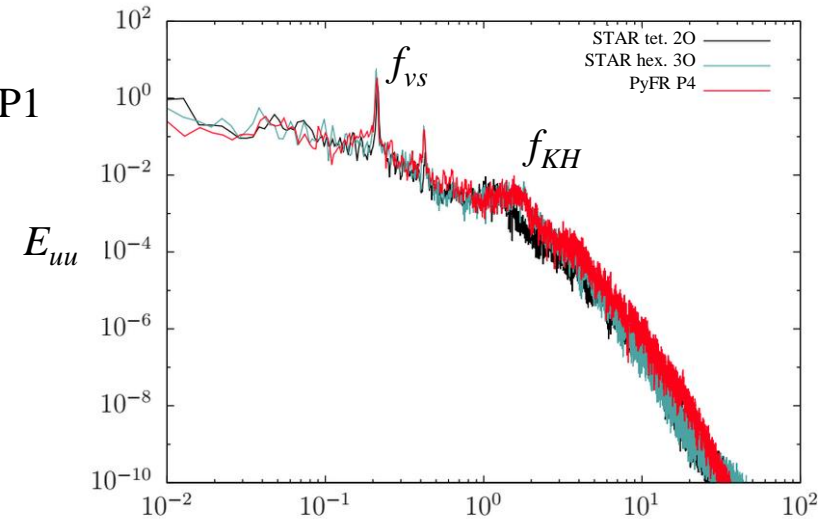
P3 DNS
(Lehmkuhl
et al., 2013)



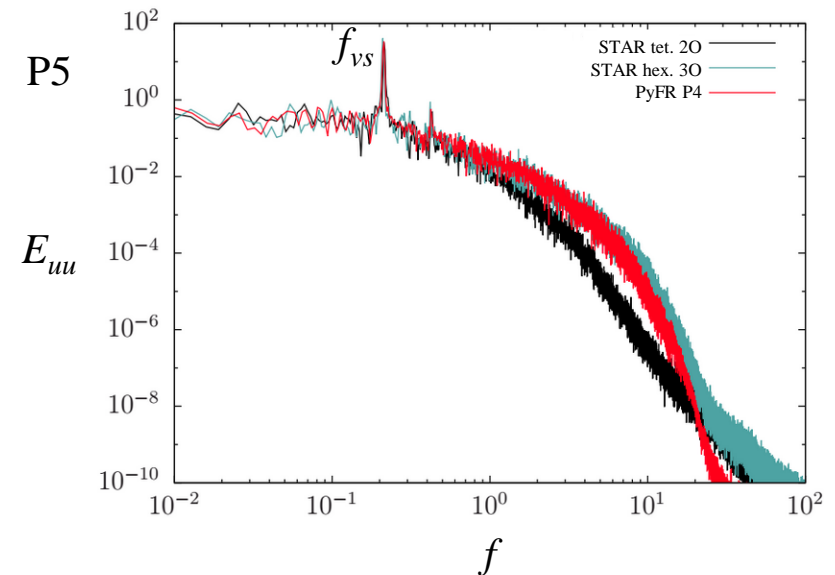
P3 30
MUSCL/CD



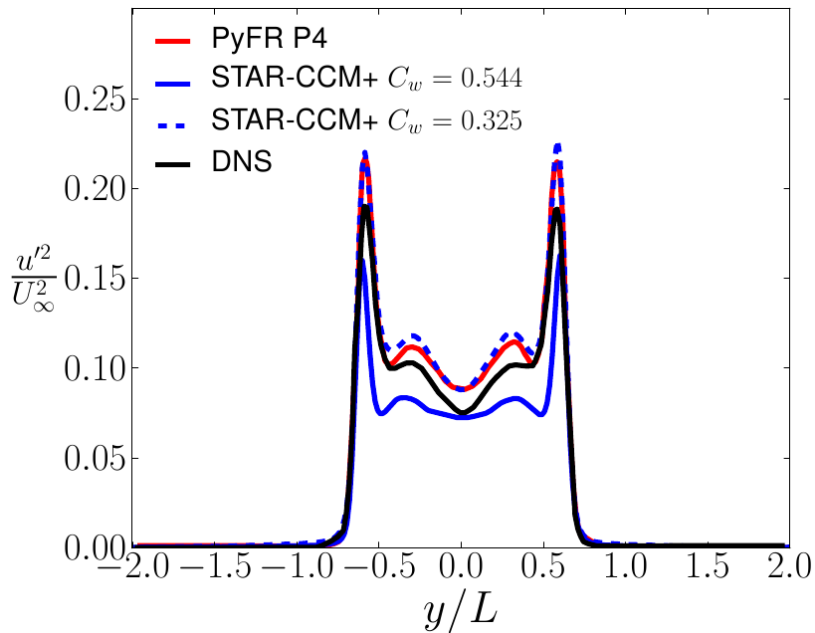
P1



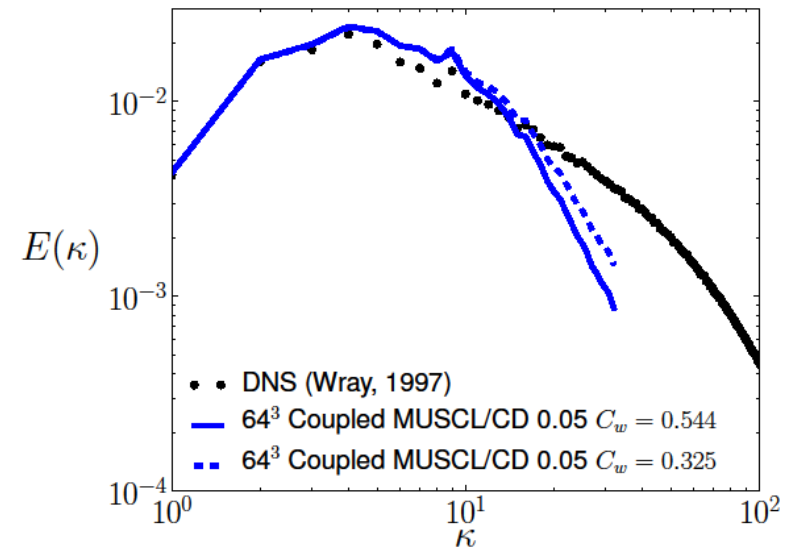
P5



LES of Circular Cylinder at Re=3,900



Effect of decreasing C_w to widely accepted value



Computational resource:

	Hardware	CUDA C Cores/core s x nodes	Price (£)	GPU/CPU hours	Resource Utilization (£xsec)
PyFR P4	Nvidia K20c GPU	2496x3x12	~2000	4.24×10^4	3.05×10^{11}
2O upwind	Xeon X5650 CPU	6 x 5	~700	6.96×10^4	1.76×10^{11}
3O MUSCL/CD	Xeon X5650 CPU	6 x 5	~700	1.39×10^5	3.51×10^{11}

Conclusions

- 3rd Order hybrid MUSCL/CD scheme was validated on fundamental test cases
- Formal order accuracy still to be proven on fundamental cases
- 3rd Order scheme compares well against higher-order codes for more complex high-fidelity simulations (both in terms of accuracy and compute resource)
- Work still needed to single out contribution to mesh and convection scheme
- Future work on proving formal convergence rate (using other HO workshop cases)

▫ Acknowledgements:

- We would like to thank B. Vermeire and P. Vincent at Imperial College for providing both 'naive-user' STAR-CCM+ settings and PyFR P4 solution for the circular cylinder.